



Royal Netherlands  
Meteorological Institute  
*Ministry of Infrastructure  
and Water Management*

# Wind across land-water transitions: Application of an analytical model to numerical model output

A. Sterl

De Bilt, 2019 | Technical report; TR-381





## Wind across land-water transitions: Application of an analytical model to numerical model output

Andreas Sterl

Koninklijk Nederlands Meteorologisch Instituut (KNMI)  
P.O. Box 201, NL-3730 AE De Bilt, Netherlands  
phone: +31-30-2206766; e-mail: sterl@knmi.nl

December 13, 2019

**Project:** Maatwerk tbv kennisontwikkeling WBI2023 en NKWK - WP3  
**Opdrachtgever:** RWS-VWL  
**Interne review:** Ine Wijnant, Andrew Stepek, and Henk van den Brink

### Abstract

To determine the wind speed over small inland water bodies, the wind measured at land stations has to be transformed to an open-water wind. The current transformation method used by Rijkswaterstaat employs the blending-height concept, which is a simplification of the Wieringa-Rijkoort Two-Layer Model. We here assess the validity of this approach by applying it to output from the high-resolution weather model HARMONIE. It turns out that the modelled winds in HARMONIE at land points and adjacent water points are not related according to the blending-height concept or the full Wieringa-Rijkoort model. Rather than using these models to infer the open-water wind, a well-calibrated and evaluated numerical atmosphere model should be used.

*Parts of this report are copied from Sterl (2018).*

# Contents

<b>Samenvatting</b>	<b>ii</b>
<b>Executive Summary</b>	<b>iii</b>
<b>1 Introduction</b>	<b>1</b>
<b>2 Theoretical background</b>	<b>1</b>
2.1 Logarithmic wind profile . . . . .	1
2.2 Drag coefficient . . . . .	2
2.3 Potential wind . . . . .	3
2.4 Current RWS-method to derive the open water wind . . . . .	3
2.5 The Wieringa-Rijkooort Two Layer Model (WR2LM) . . . . .	5
<b>3 The HARMONIE model</b>	<b>6</b>
3.1 Model description . . . . .	6
3.2 Earlier results using HARMONIE . . . . .	7
3.3 Vertical profiles in HARMONIE . . . . .	7
<b>4 Performance of the Blending Height Model</b>	<b>9</b>
4.1 Transformation to neighbouring points . . . . .	9
4.2 Transformation over larger distances . . . . .	12
4.3 Reasons for failure . . . . .	12
4.3.1 Blending height . . . . .	12
4.3.2 Macro wind . . . . .	15
<b>5 Discussion</b>	<b>18</b>
5.1 The theory behind the WR2LM . . . . .	18
5.2 The WR2LM . . . . .	18
5.3 The curvature problem . . . . .	19
<b>6 Summary and conclusion</b>	<b>19</b>
<b>References</b>	<b>20</b>

## Samenvatting

Voor vele veiligheidstoepassingen (bv. golfhoogtes of wateropstuwing door wind) is kennis van de wind boven water (bv. grote meren) vereist. Meestal wordt de wind echter alleen op land gemeten, en de open water wind wordt uit de gemeten landwind afgeleid. Rijkswaterstaat (RWS) gebruikt hiervoor het Blending Height Model (BHM): Aangenomen wordt dat de wind op 60 m hoogte (de *blending height*) onafhankelijk is van de lokale oppervlakterutheid en dus niet beïnvloed wordt door de overgang van land naar water. Het BHM is een vereenvoudiging van het Wieringa-Rijkooort Two-Layer Model (WR2LM). In het WR2LM wordt aangenomen dat niet de wind op de blending height, maar de wind aan de bovenkant van de Ekmanlaag over het water geëxtrapoleerd kan worden.

Een eerder rapport (Sterl 2018; KNMI TR-363) liet zien dat de aanname niet klopt dat de wind op 60 m hoogte door de land-water overgang niet beïnvloed wordt. We onderzoeken deze aanname hier in meer detail en laten zien dat dat toepassing van het BHM niet tot de correcte wind over open water leidt. We onderzoeken verder ook het WR2LM en vinden dat ook de wind aan de bovenkant van de Ekmanlaag niet over de land-water grens geëxtrapoleerd mag worden. Het gebruik van het WR2LM voor de extrapolatie van wind van land naar water werd al door de bedenkers van dat model afgeraden. Het door hun beoogde gebruik was voor de interpolatie tussen waarneemstations.

Het onderzoek is gebaseerd op de uitvoer van HARMONIE. Dat is een niet-hydrostatisch numeriek weermodel met een hoge resolutie (2,5 km), dat door het KNMI voor de dagelijkse weerverwachting gebruikt wordt. De basisaanname is dus dat de HARMONIE uitvoer de processen in de grenslaag en de resulterende windprofielen correct beschrijft, met name over land-water grenzen heen. Een vergelijking tussen waargenomen en gemodelleerde windprofielen over land en over zee laat een goede overeenstemming zien. Hieruit concluderen we dat het model de grenslaagprocessen goed weergeeft, en dat de modeluitvoer dus gebruikt kan worden om de aannames achter het BHM en het WR2LM te testen.

We concluderen dat het BHM noch het complete WR2LM de windveranderingen bij de overgang van land naar water correct weergeven. Ze zouden dus niet moeten worden gebruikt om de over land gemeten wind naar wind over open water om te rekenen. Het is beter om de open-water wind met een goed gekalibreerd en gevalideerd numeriek atmosfeermodel te bepalen.

## Executive Summary

For a lot of safety-relevant applications (e.g., wave height, wind set-up) the wind over water (e.g. large lakes) is needed. However, measurement stations are usually situated on land, and the wind over water has to be derived from the wind over land. This is done by Rijkswaterstaat with the Blending Height Model (BHM). The basic assumption of the BHM is that the wind at the *blending height* of 60 m is independent of the local roughness and is therefore not influenced by the land-water transition. The BHM is a simplification the Wieringa-Rijkoort Two-Layer Model (WR2LM), which assumes that the wind at the top of the Ekman layer, rather than the wind at the blending height, may be extrapolated across the land-water boundary.

In an earlier report (Sterl 2018; KNMI TR-363) it was briefly shown that the assumption of the wind being constant across land-water boundaries at 60 m height is not valid. We here investigate that assumption in more detail and show that the BHM does not lead to the correct open water wind. We also investigate the WR2LM and find that also the wind at the top of the Ekman layer may not be extrapolated across the land-water boundary. The use of the WR2LM to extrapolate the wind from land to water was already discouraged by the developers of that model. Rather, they recommended it to interpolate between adjacent stations.

The investigation is based on the output of HARMONIE, a high-resolution (2.5 km) non-hydrostatic numerical weather forecast model, that is used operationally by KNMI. Thus the basic assumption is that the HARMONIE output correctly describes the boundary-layer processes and the resulting wind profiles, especially across land-water boundaries. A comparison between observed and modelled wind profiles over land and over water shows a good correspondence, suggesting that the model output correctly describes the boundary-layer processes and can be used to test the assumptions behind the BHM and the WR2LM.

We conclude that neither the BHM nor the full WR2LM describe the transition of the wind at land-water boundaries correctly. They should not be used to transform the measured wind over land to wind over open water. Instead, a well-calibrated and evaluated numerical atmosphere model should be used to infer the open-water wind.

# 1 Introduction

For a lot of safety-relevant applications (e.g., wave height, wind set-up) the wind over water (e.g. large lakes) is needed. However, measurement stations are usually situated on land. To derive the open water wind over small inland water bodies from nearby wind measurements on land, Rijkswaterstaat (RWS) use a method that essentially assumes that the wind at the *blending height* of 60 m height is independent of the local roughness and can be assumed constant over large distances (sometimes tens of kilometres). However, based on a simple model for the growth of an internal boundary layer, Bottema (2007) (his Appendix E) argues that this assumption already breaks down for distances  $\gtrsim 1$  km. Using model output, Sterl (2018) shows that the wind at 60 m height changes quite abruptly at the land-water boundary, corroborating the result of Bottema (2007). Figure 3 of Sterl (2018), showing the abrupt change, is reproduced here for convenience (Fig. 1).

We here investigate the validity of the RWS approach in more detail by applying it to output of the numerical weather forecast model HARMONIE (Bengtsson et al., 2017). This model is used operationally at KNMI at a horizontal resolution of 2.5 km, allowing the larger inland water bodies to be resolved (see Fig. 2). This makes it possible to compare the winds obtained by applying the blending height assumption with those simulated by HARMONIE.

## 2 Theoretical background

### 2.1 Logarithmic wind profile

The wind profile of a turbulent flow above a rough surface is logarithmic (e.g., Tennekes, 1973):

$$U(z) = \frac{u_*}{\kappa} \ln \left( \frac{z}{z_0} \right), \quad (1)$$

where  $u_* = \sqrt{\tau/\rho_a}$  is the friction velocity,  $\kappa = 0.41$  the von Kármán constant<sup>2</sup>, and  $z_0$  the roughness length. The roughness length is a characteristic of the surface conditions in a certain area around the measurement site.  $\tau$  and  $\rho_a$  are respectively the wind stress and the air density.

<sup>1</sup>Please note that in all plots some of the smaller islands in the Wadden Sea and the Rhine-Meuse delta are missing. They are not present in the database of the plot program used.

<sup>2</sup>Note that some authors use  $\kappa = 0.4$ . However, the exact value of  $\kappa$  is not important here as long as the same values is used throughout.

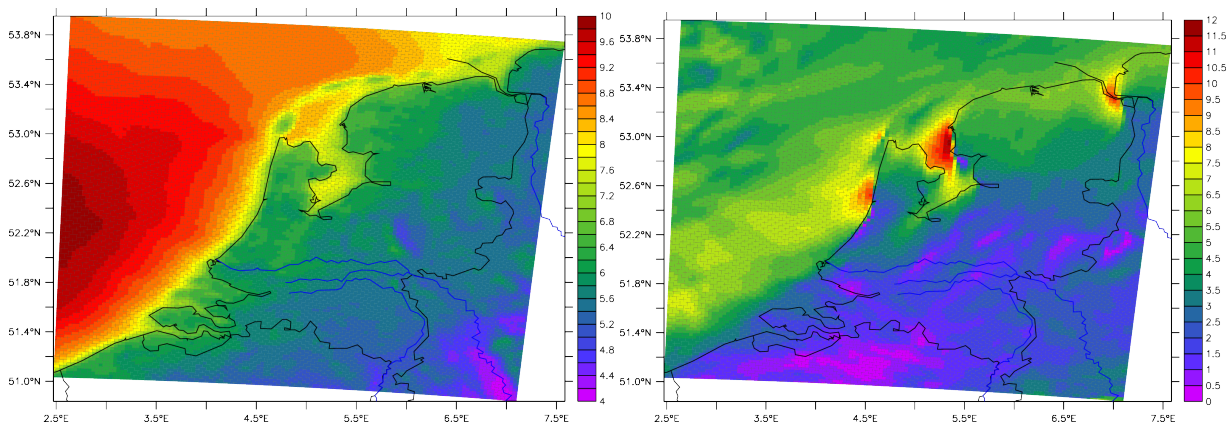


**Figure 1:** 60-m wind from a run using the high-resolution (2.5 km) HARMONIE model for May 2012). Left: monthly average, right: May 16, 11.00 hours. Note the different scales in both plots.<sup>1</sup> (Reproduced from Sterl, 2018.)

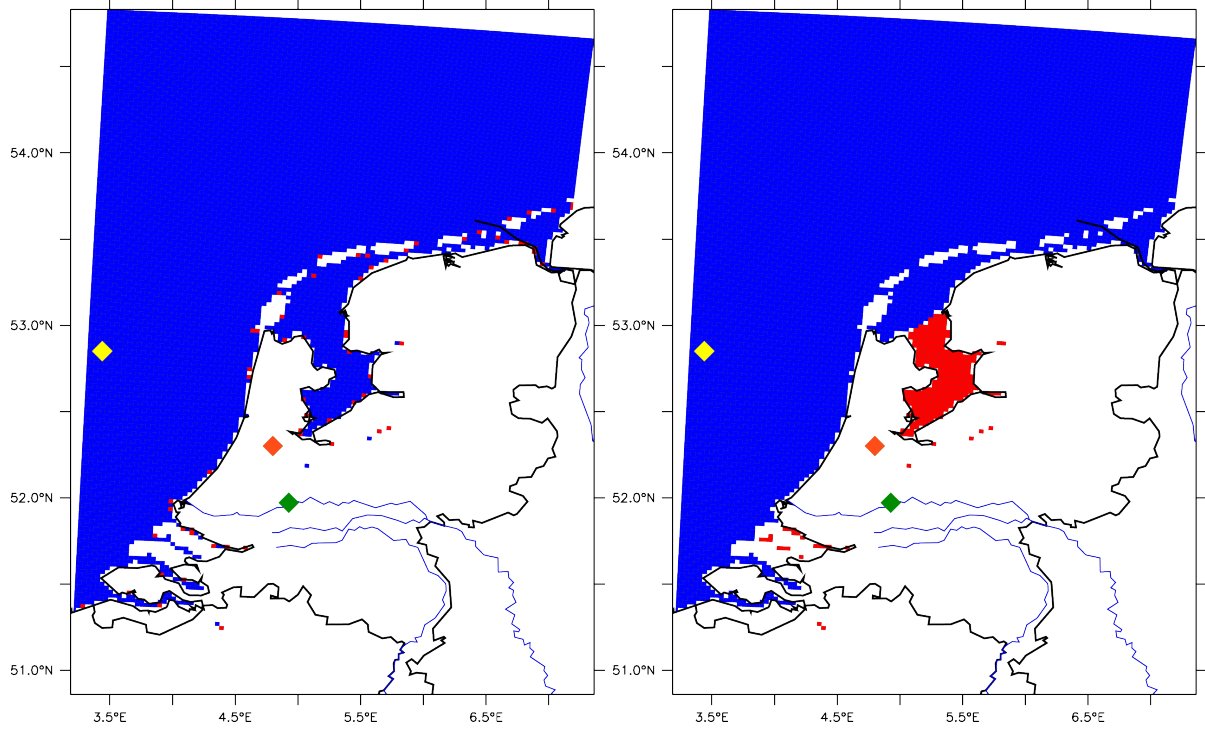


**Figure 2:** Surface characteristics of HARMONIE over the Netherlands. **Left:** Grid boxes which consist for more than 90% of water are in blue, and those with 80-90% of water in red. **Right:** Distinction between water types. Grid boxes which consist of more than 80% of *sea* are in blue, those that consist of more than 80% of *lake* are in red. The positions Meteomast IJmuiden, Schiphol and Cabauw are indicated by respectively the yellow, orange and green diamonds.

Applying (1) at two different heights  $z_1$  and  $z_2$  yields

$$U(z_1) = U(z_2) \frac{\ln\left(\frac{z_1}{z_0}\right)}{\ln\left(\frac{z_2}{z_0}\right)}. \quad (2)$$

Eq. (1) is only valid for a neutrally stratified atmosphere. For non-neutral conditions the equation has to be modified to

$$U(z) = \frac{u_*}{\kappa} \left( \ln\left(\frac{z}{z_0}\right) - \Psi(\zeta) \right), \quad (3)$$

where  $\Psi$  is the stability function,  $\zeta = z/L$  is the non-dimensional stability parameter, and  $L$  is the Obukhov length. The atmosphere is stable (unstable) for  $\zeta > 0$  ( $< 0$ ).

## 2.2 Drag coefficient

The stress  $\tau$  exerted by the wind on the surface is usually parameterized as

$$\tau = \rho_a u_*^2 = \rho_a C_{D,z} U(z)^2, \quad (4)$$

where  $C_{D,z}$  is the drag coefficient for height  $z$ . Usually,  $z = 10$  m is used as the reference height, and  $C_{D,10}$  is abbreviated as  $C_D$ . Combining the logarithmic profile (1) with the definition of the drag coefficient (4) and putting  $U(10) = U_{10}$  results in

$$C_D = \left( \frac{u_*}{U_{10}} \right)^2 = \frac{\kappa^2}{\ln^2\left(\frac{10}{z_0}\right)}. \quad (5)$$

The roughness length over water is usually parameterized as

$$z_0 = 0.1 \frac{\nu}{u_*} + \alpha \frac{u_*^2}{g}, \quad (6)$$

where  $\nu$  is the kinematic viscosity of air,  $g$  the acceleration due to gravity, and  $\alpha$  the Charnock parameter. The first term describes the viscous stress and is only relevant at low wind speeds.

### 2.3 Potential wind

Wind measurements over land are usually performed at a height of  $z_{\text{obs}} = 10$  m, but other heights are possible. To make these winds comparable, they are transformed to the common *reference height*  $z_{\text{ref}} = 10$  m. Furthermore, typical measurement heights are relatively close to the surface. Each measurement location has its own characteristic surface roughness which directly impacts the measured wind  $U_{\text{obs}}$ . Measured winds are therefore not representative for a wider area or for winds at greater heights. To make measured winds comparable between locations, they are transformed to the *potential wind*  $U_{\text{pot}}$  (Wieringa and Rijkoort, 1983; Wieringa, 1986). This is the wind that would have been measured at  $z_{\text{ref}} = 10$  m if the local roughness had been that of flat grassland. The corresponding roughness length  $z_{0,\text{ref}} = 0.03$  m is used as the *reference roughness* (see Fig. 3).

The potential wind is determined by first using (2) to transform the observed wind  $U_{\text{obs}}$  to  $U_{\text{bld}}$ , the wind at the *blending height*  $z_{\text{bld}} = 60$  m, where the wind speed (*meso wind*) is assumed to be independent of the local surface roughness. In this transformation the actual local roughness  $z_{0,l}$  at the measurement site is used. In a second step,  $U_{\text{bld}}$  is transformed back to the reference height  $z_{\text{ref}}$ . Again (2) is used, but with the reference roughness  $z_{0,\text{ref}}$ ,

$$U_{\text{bld}} = U_{\text{obs}} \frac{\ln\left(\frac{z_{\text{bld}}}{z_{0,l}}\right)}{\ln\left(\frac{z_{\text{obs}}}{z_{0,l}}\right)}, \quad (7a)$$

$$U_{\text{pot}} = U_{\text{bld}} \frac{\ln\left(\frac{z_{\text{ref}}}{z_{0,\text{ref}}}\right)}{\ln\left(\frac{z_{\text{bld}}}{z_{0,\text{ref}}}\right)} \quad (7b)$$

$$= U_{\text{obs}} \frac{\ln\left(\frac{z_{\text{bld}}}{z_{0,l}}\right)}{\ln\left(\frac{z_{\text{obs}}}{z_{0,l}}\right)} \cdot \frac{\ln\left(\frac{z_{\text{ref}}}{z_{0,\text{ref}}}\right)}{\ln\left(\frac{z_{\text{bld}}}{z_{0,\text{ref}}}\right)}. \quad (7c)$$

Equation (7b) shows that  $U_{\text{pot}}$  and  $U_{\text{bld}}$  have a constant ratio. Inserting the standard values ( $z_{\text{ref}} = 10$  m,  $z_{0,\text{ref}} = 0.03$  m,  $z_{\text{bld}} = 60$  m) yields  $U_{\text{pot}} = 0.764 \cdot U_{\text{bld}}$ .

### 2.4 Current RWS-method to derive the open water wind

For practical reasons wind measurements are usually done over land. Although measurements over water do exist (e.g., see Fig. 4.3 in Baas, 2014), they are usually of short duration, not allowing to derive robust statistics. To drive their hydraulic models, RWS use statistical distributions of  $U_{\text{pot}}$  that are derived from measurements at nearby KNMI land stations and transformed into wind over open water. These distributions form the basis for their assessment of coastal defence structures.

The basic assumption in the current RWS-method to derive the open water wind is that  $U_{\text{bld}}$  is the same over land and the adjacent water. In other words, the wind at the blending height does not “feel” the land-water boundary. We will refer to this assumption as the *Blending Height Model* (BHM). With this assumption the open water wind  $U_{\text{ow}}$  is obtained by first transforming the potential wind back to the blending height using the reference roughness  $z_{0,\text{ref}}$ , and then

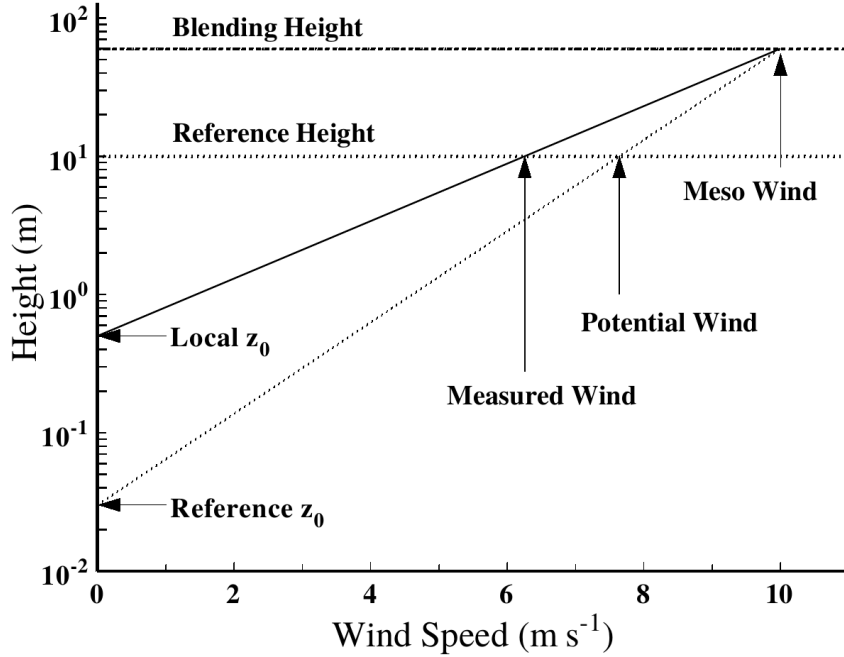


**Figure 3:** Potential wind speed: From the measured wind speed and the local roughness length, the wind speed at the blending height is computed. This *meso wind* speed is translated downward to the potential wind speed at the reference height and with reference roughness length. In this plot the measuring height ( $z_{\text{obs}}$ ) and the reference height ( $z_{\text{ref}}$ ) are both 10 m, the blending height is 60 m, the local roughness length is 0.5 m, and the reference roughness length is 0.03 m. The height transformations are done using the logarithmic wind speed profile. (Copied from Verkaik, 2006.)

again down to  $z_{\text{ref}} = 10$  m using the wind-dependent (see recent review of Sterl, 2017) roughness length  $z_{0,\text{ow}}$  of open water. Applying (2) twice as in section 2.3 yields

$$U_{\text{ow}} = U_{\text{pot}} \frac{\ln\left(\frac{z_{\text{bld}}}{z_{0,\text{ref}}}\right)}{\ln\left(\frac{z_{\text{ref}}}{z_{0,\text{ref}}}\right)} \cdot \frac{\ln\left(\frac{z_{\text{ref}}}{z_{0,\text{ow}}}\right)}{\ln\left(\frac{z_{\text{bld}}}{z_{0,\text{ow}}}\right)}. \quad (8)$$

Inserting (7c) yields

$$U_{\text{ow}} = U_{\text{obs}} \frac{\ln\left(\frac{z_{\text{bld}}}{z_{0,l}}\right)}{\ln\left(\frac{z_{\text{obs}}}{z_{0,l}}\right)} \cdot \frac{\ln\left(\frac{z_{\text{ref}}}{z_{0,\text{ow}}}\right)}{\ln\left(\frac{z_{\text{bld}}}{z_{0,\text{ow}}}\right)}, \quad (9)$$

showing that this is equivalent to skipping the calculation of the potential wind and directly transform the observed wind  $U_{\text{obs}}$  to the open water wind using the open water roughness  $z_{0,\text{ow}}$ . The use of the potential wind has practical reasons. It is independent of the local situation at the measurement site. Equation (9) is the mathematical implementation of the BHM.

The open water roughness length is calculated from (5) as

$$z_{0,\text{ow}} = 10 e^{-\kappa/\sqrt{C_D}}, \quad (10)$$

where the drag coefficient  $C_D$  is assumed to increase linearly with  $U_{10} = U_{\text{ow}}$  according to Wu (1982). Therefore the roughness length depends on wind speed, and (9) and (10) are implicit equations for  $U_{\text{ow}}$  and the drag coefficient (and thus the stress) that need to be solved iteratively.

The transformation process does not involve stability corrections, but assumes neutral stability. This choice is motivated by the interest in safety-relevant cases, i.e., high wind speeds. Under high wind speeds, turbulence usually prevents stratification. However, Caires et al. (2012)

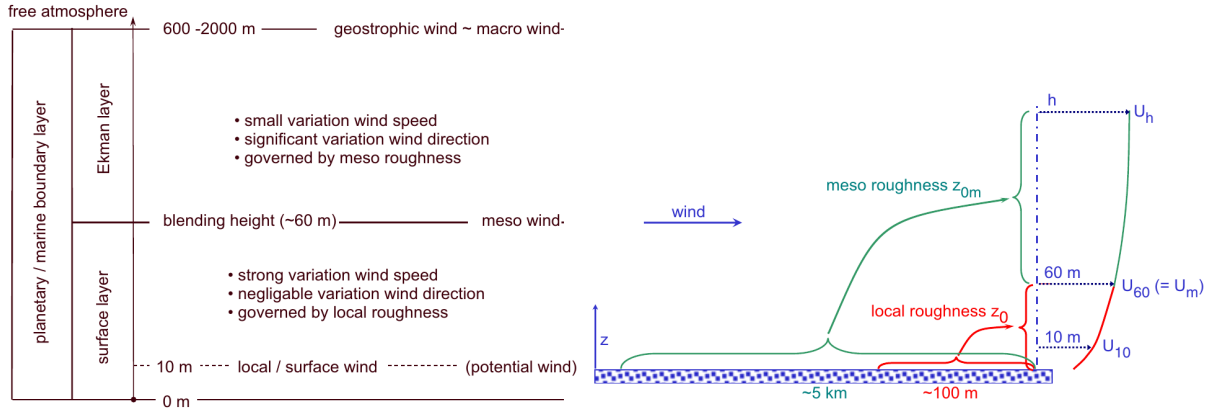


**Figure 4:** *Left:* Schematized properties of the wind in the WR2LM. *Right:* Relation between surface roughness and the wind speed profile, subdivided in two layers.  $U$  indicates wind speed, the subscript “m” stands for *meso*, and  $h$  is the height of the upper boundary of the Ekman layer ( $= h_{ek}$  in the text). (Copied from Caires et al., 2012.)

present evidence that stability effects can play a role even at high wind speed. In this report we do not investigate this aspect further, but apply the transformation under the usual assumption of neutral stability.

## 2.5 The Wieringa-Rijkoort Two Layer Model (WR2LM)

The assumption of a blending height at which the wind is independent of the local roughness is a simplification of the Wieringa-Rijkoort Two Layer Model (WR2LM) (Wieringa and Rijkoort, 1983; Wieringa, 1986). That model assumes two layers, one extending from the surface to the blending height, and the second one from the blending height to the height of the Ekman layer (Fig. 4). Below the blending height, the wind is governed by the local roughness  $z_{0,l}$ , which is characteristic for an upstream distance of a few hundred metres. Above the blending height, the wind is no longer influenced by the local roughness, but by the *meso roughness*  $z_{0,m}$ , which is representative for an upstream distance of a few kilometres. Wieringa and Rijkoort (1983) recommend an upstream area of  $5 \text{ km} \times 5 \text{ km}$  to determine the meso roughness.

As the wind speed must be continuous across the boundary between the two layers, both roughness values must lead to the same velocity at the blending height, so from (1) we get

$$U_{\text{bld}} = \frac{u_*}{\kappa} \ln \left( \frac{z_{\text{bld}}}{z_{0,l}} \right) = \frac{u_{*,m}}{\kappa} \ln \left( \frac{z_{\text{bld}}}{z_{0,m}} \right), \quad (11)$$

where  $u_*$  and  $u_{*,m}$  are the friction velocities determined from the local and the meso roughness, respectively.

Within the Ekman layer the wind is governed by the laws of geostrophic resistance, and its direction changes with height. At the top of the Ekman layer, the wind components relative to the surface wind direction are given by (Blackadar and Tennekes, 1968; Tennekes, 1973)

$$U_h = \frac{u_{*,m}}{\kappa} \ln \left( \frac{h_{ek}}{z_{0,m}} \right) = U_{\text{bld}} + \frac{u_{*,m}}{\kappa} \ln \left( \frac{h_{ek}}{z_{\text{bld}}} \right), \quad (12a)$$

$$V_h = \frac{u_{*,m}}{\kappa} B, \quad (12b)$$

where  $A = 1.9$  and  $B = 4.5$  are two empirical constants, and

$$h_{ek} = u_{*,m} / (f e^A) \quad (13)$$

is the height of the Ekman layer, with  $f$  the Coriolis parameter ( $1.17 \cdot 10^{-4} \text{ s}^{-1}$  at  $53^\circ\text{N}$ ). The second equality in (12a) results from the second equality in (11). Finally, the wind speed at the top of the Ekman layer, also called the *macro wind speed*, is given by

$$S_h = \sqrt{U_h^2 + V_h^2}. \quad (14)$$

To use this two layer model to infer the open-water wind from wind measurements done over land, it is assumed that  $S_h$  and its components  $U_h$  and  $V_h$  are spatially slowly varying, so that they (rather than the meso wind!) can be extrapolated from the measurement position. The open-water wind is thus calculated by the following procedure:

1. Calculate  $U_{\text{bld}}$  from (7a), using the measured wind,  $U_{\text{obs}}$ , and the local roughness,  $z_{0,l}$ .
2. Calculate  $u_{*,m}$  from the second part of (11), using  $U_{\text{bld}}$  and the meso roughness,  $z_{0,m}$ .
3. Calculate  $U_h$  from the first part of (12a), using  $u_{*,m}$ .
4. Shift the calculated value of  $U_h$  to the desired open-water position.
5. At this position, determine  $u_{*,m}^{\text{ow}}$  from the corresponding meso roughness  $z_{0,m}^{\text{ow}}$  and  $U_h$ , using the first part of (12a). As  $h_{\text{ek}}$  depends on  $u_{*,m}$  (eq. 13), this is an implicit relation that has to be solved iteratively.
6. Calculate  $U_{\text{bld}}^{\text{ow}}$  from the second part of (12a), using  $U_h$  and  $u_{*,m}^{\text{ow}}$ .
7. Calculate the near-surface wind speed  $U_{\text{ref}}^{\text{ow}}$  from (7a), using  $U_{\text{bld}}^{\text{ow}}$  and  $z_{0,l} = z_{0,l}^{\text{ow}}$ .

It is easy to see that within the framework of the WR2LM the following two assumptions are equivalent, (i) the BHM is valid,  $U_{\text{bld}}^{\text{ow}} = U_{\text{bld}}$ , and (ii) the two sites are influenced by the same meso roughness,  $z_{0,m}^{\text{ow}} = z_{0,m}$ . The implication (ii)  $\Rightarrow$  (i) shows that the BHM is a simplification of the WR2LM for the case that the two sites are governed by the same meso roughness. The equivalence between constant meso roughness and constant meso wind (i.e., the BHM) gives an indication why the BHM might fail: if the meso roughness is not constant, e.g., at a land-water transition, the meso wind cannot be constant either.

## 3 The HARMONIE model

### 3.1 Model description

We here use output from a climate version of HARMONIE. The model domain consists of  $789 \times 789$  grid points and is centered on Utrecht (Netherlands). Having a horizontal resolution of 2.5 km, it covers most of western Europe. At the lateral boundaries atmospheric conditions are prescribed from the ERA-Interim reanalysis (Dee et al., 2011) that are updated every 6 hours. Away from the boundaries, the model is running freely, without any data assimilation. The model adapts to the prescribed conditions within a few grid rows along the boundaries. As the Netherlands are 800–1000 km away from the boundaries, any disturbances generated there have died out. The model is run over the period 2005–2014.

The run analyzed here uses model version HCLIM38h1. In contrast to earlier versions the turbulence is parameterized with a scheme developed for the RACMO regional climate model (Lenderink and Holtslag, 2004). This HARATU (HARMONIE with RACMO TUrbulence) scheme leads to much better wind profiles in the lower atmosphere (Bengtsson et al., 2017; de Rooy and de Vries, 2017). In particular, the slope of the wind profile is very close to that of observed profiles, and the shear correction applied by Geertsema and Van den Brink (2014) is no longer necessary (see Sect. 3.3).

The model distinguishes between several surface types, among them two types of water, namely *sea* and *lake* (Fig. 2, right). At sea points, the surface temperature is prescribed (also from ERA-Interim), while at lake points it is calculated by the model. All surface processes, including the fluxes, are handled by the SURFEX package (Masson et al., 2013), which offers a choice of different parameterizations. In the configurations used in HARMONIE, the ECUME model is used at sea points. ECUME is a bulk formulation to calculate the turbulent fluxes. It employs a stability correction and a wind-speed dependent neutral drag coefficient. The drag coefficient is fitted to several measurement campaigns and flattens off for wind speeds above  $\approx 25$  m/s (see for instance Van den Brink et al., 2013). Over lake surfaces a simple Charnock relation (6) is used with  $\alpha = 0.015$  and the viscosity term neglected.

### 3.2 Earlier results using HARMONIE

The HARMONIE model has been thoroughly evaluated against observations. These investigations have been done with earlier versions of the model, and it is not known to what extent their conclusions are still valid for the present version, and a re-evaluations is beyond the scope of this report. However, as the model is constantly validated against observations, we can safely assume that it is not deteriorating. The main findings relevant for land-water transitions are

- The model is able to reproduce the large-scale structure of the wind fields both in space and time Baas and de Waal (2012).
- Wind speeds over the Netherlands are slightly overestimated by HARMONIE, especially at high wind speeds Baas (2014).
- The development of the wind field behind a land-water transition is better captured by HARMONIE than by the WR2LM (Baas and de Waal, 2012).
- While the development of the wind profile behind a land-water transition is well modelled in unstable conditions, it is too slow in neutral and stable conditions (Baas, 2014).
- The modelled wind profile over land is too steep (Geertsema and Van den Brink, 2014). This problem has been solved by the introduction of the HARATU parametrization (Bengtsson et al., 2017; de Rooy and de Vries, 2017; and Sect. 3.3).

Because of its generally good performance, the model has been used extensively to investigate and describe the wind climate of the Netherlands and the North Sea. The well-known KNMI North Sea Wind (KNW) atlas (<http://projects.knmi.nl/knw>) and its successor, the Dutch Offshore Wind Atlas (DOWA) (<https://www.dutchoffshorewindatlas.nl>) are based on HARMONIE output, as is the 100-m wind map of Geertsema and Van den Brink (2014).

### 3.3 Vertical profiles in HARMONIE

We now compare modelled and observed vertical profiles of wind speed at two locations, one at land and one over sea. The land site is the Cabauw tower (4.927°E, 51.971°N), the sea site the Meteomast IJmuiden (3.44°E, 52.85°N). Both positions are indicated in Fig. 2. The Cabauw tower is a 200 m tall tower equipped with meteorological instruments. The site is situated in a flat terrain to the south-west of Utrecht, that mainly consists of grassland. The Meteomast IJmuiden was operated from 2013 to 2015 (Kalverla et al., 2017). It is situated about 85 km off the Dutch coast. It is 90 m tall and equipped with anemometers at different heights, and an upward looking Lidar at the top measuring wind speed and direction up to a height of 315 m.

Figure 5 depicts vertical profiles of observed and modelled winds at the Cabauw tower for two different months. The monthly-mean difference between the two is very small. Above a height of 20 m both observed and modelled profiles are logarithmic with the same slope. The

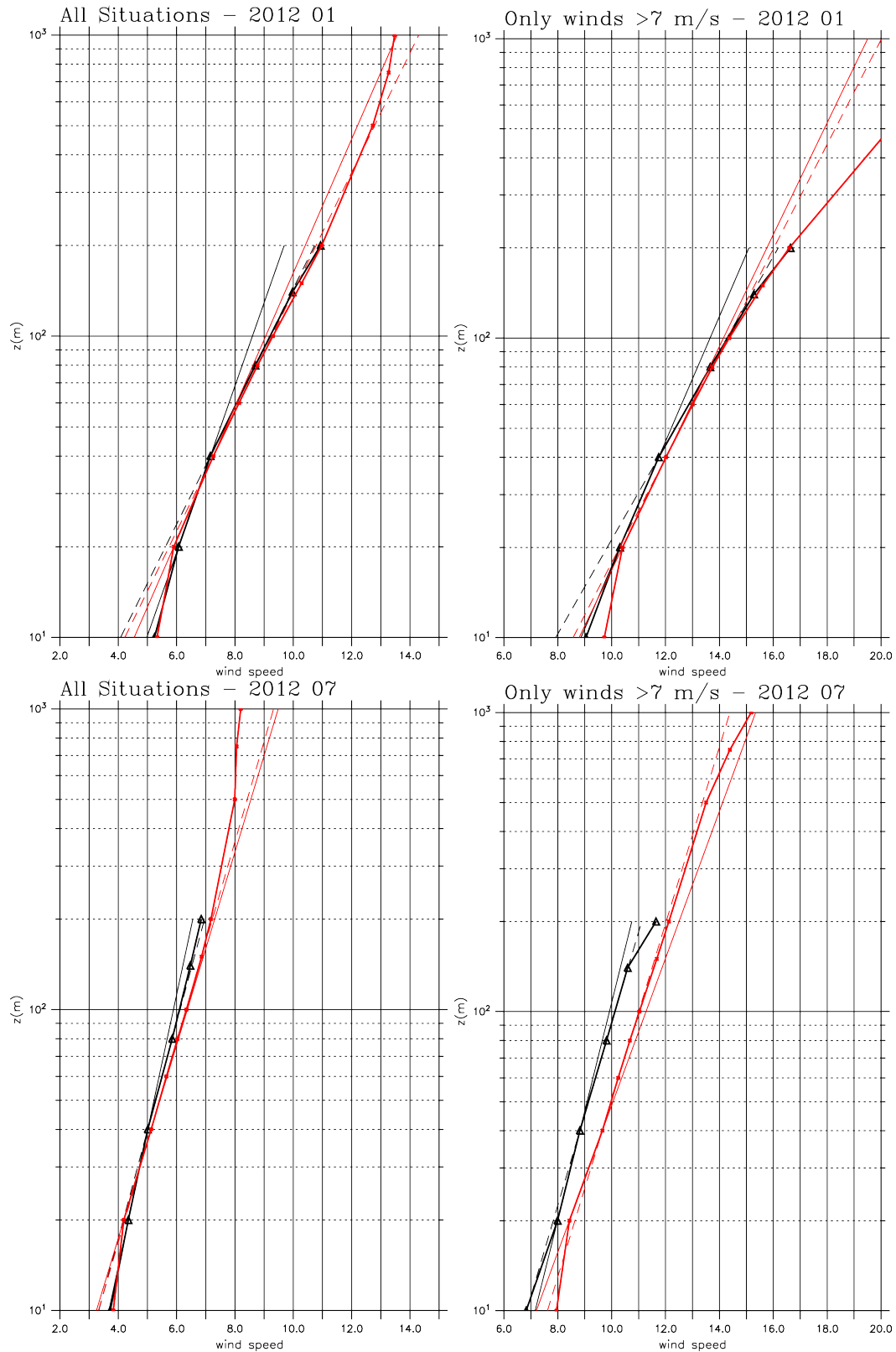


**Figure 5:** Observed (black) and modelled (red) wind profiles at the Cabauw tower in January (upper row) and July (lower row) of 2012, divided into all situations (left) and high-wind ( $U_{10} > 7$  m/s) situations (right). The thick lines connect the observed (modelled) wind speeds at the measurement (output) heights (markers). The thin solid (dashed) lines represent a fit (linear in  $\ln z$ ) to the values at 40 m and 20 m (80 m and 40 m).

difference for the high-wind cases in July is mainly caused by a sampling issue: there are just a few such cases in July. In earlier model versions the slope was smaller than in the observations (see Geertsema and Van den Brink, 2014). The improvement is due to the adoption of the HARATU turbulence scheme.

Both observed and modelled 10 m winds are higher than suggested by a linear (linear in  $\ln z$ ) downward extrapolation of the profiles from heights above 20 m. The linear extrapolations are shown in Fig. 5 by the thin lines, which depict fits to the values at 40 m and 20 m (continuous lines) and 80 m and 40 m (dashed lines). Averaged over a whole month, modelled and observed 10 m winds agree well with each other, but at high winds the modelled 10 m winds are higher than the observations, and the overestimation relative to the linear fit is larger. The deviation of the profile from logarithmic below 20 m has been observed before (e.g., Verkaik and Holtslag (2007) and references therein). The reason is that at heights exceeding  $\approx 20$  m the wind profile is already influenced by larger roughness elements upstream of the measuring site, while below that height it is only influenced by the local roughness (flat grassland in case of the Cabauw site). The feature is not a model artifact, and its reproduction by the model strengthens our confidence in the model's quality. That the deviation is smaller in the model than in the observations is due to the size of the model grid. At a grid size of  $2.5 \text{ km} \times 2.5 \text{ km}$ , the roughness is not representative for the local conditions at the measurement site, but influenced by obstacles farther away.

Figure 6 shows similar plots for the sea site of Meteomast IJmuiden. Also these profiles are logarithmic, with identical slopes for observations and model output. During winter, the model overestimates the observed wind speed by about 10%. As for the land site, the modelled 10 m wind is larger than suggested by an extrapolation of the logarithmic slope towards the surface, but the deviation is much smaller.

At both locations the monthly-mean profiles are logarithmic (Figs. 5 and 6). However, individual profiles, both observed and modelled, can deviate significantly from the logarithmic form. For the Meteomast IJmuiden such non-logarithmic profiles have been classified and investigated by Kalverla et al. (2017).

As observed and modelled wind speed profiles at the two locations agree very well, we can use the model output to test the performance of the transformation (9). This is done in the next section.

## 4 Performance of the Blending Height Model

### 4.1 Transformation to neighbouring points

As explained in Sect. 2.4, RWS use the BHM (9) to determine the wind over open water from measured wind at a nearby land point. We now test how well this procedure would work in HARMONIE. To do so, we try to determine the 10 m wind at the point *to the east* of each grid point by putting  $z_{0,ow} = z_0(i+1)$  in eq. (9), i.e.,

$$\hat{U}_{\text{ref}}(i+1) = U_{\text{obs}}(i) \frac{\ln\left(\frac{z_{\text{bld}}}{z_0(i)}\right)}{\ln\left(\frac{z_{\text{obs}}}{z_0(i)}\right)} \cdot \frac{\ln\left(\frac{z_{\text{ref}}}{z_0(i+1)}\right)}{\ln\left(\frac{z_{\text{bld}}}{z_0(i+1)}\right)}, \quad (15)$$

where  $i$  is the x-index of the base point. So if point  $i$  is a land point and point  $i+1$  a water point (e.g., western shore of Lake IJssel), we follow the recipe (9) to determine the open water wind. In the opposite case ( $i$  water and  $i+1$  land; eastern shore of Lake IJssel and North Sea coast) we apply essentially the same equation, but transforming the wind from water to land.  $\hat{U}_{\text{ref}}$  according to (15) is then compared to the modelled value  $U_{\text{ref}}$ .

The result of this exercise is presented in Fig. 7a. Clearly, the wind speed is underestimated (by  $\approx 0.5 \text{ m/s}$ ) if the transformation is done from land to water (western shore of Lake IJssel), and overestimated in the opposite case. To avoid possible problems arising from grid points being

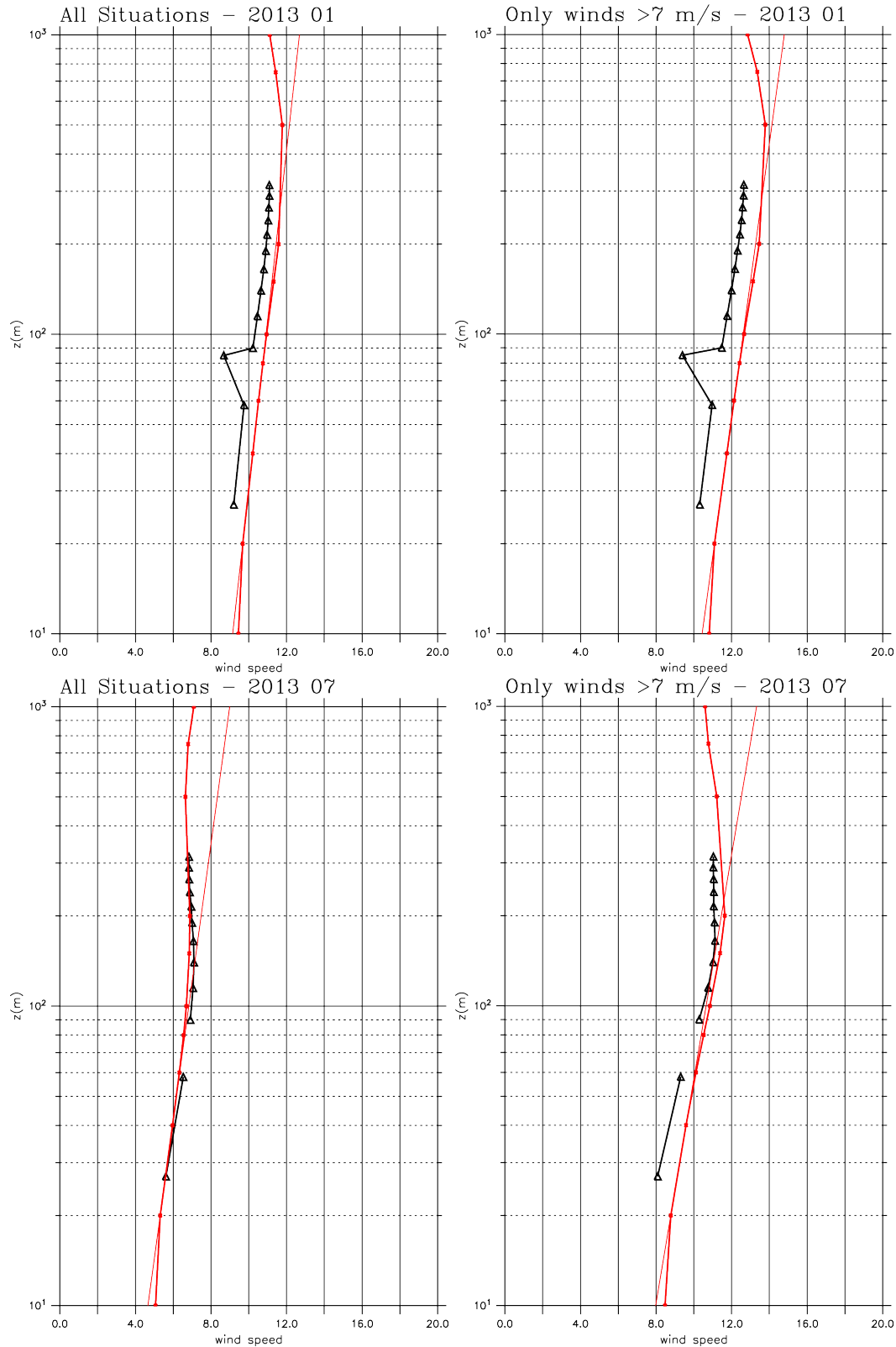


**Figure 6:** Observed (black) and modelled (red) wind profiles at Meteomast IJmuiden in January (upper row) and July (lower row) of 2013, divided into all situations (left) and high-wind ( $U_{10} > 7$  m/s) situations (right). The thick lines connect the observed (modelled) wind speeds at the measurement (output) heights (markers). The thin solid lines represent a fit (linear in  $\ln z$ ) to the modelled values at 40 m and 20 m. Note that there are many missing values at the 87 m measurement height, causing a large deviation between modelled and observed values.

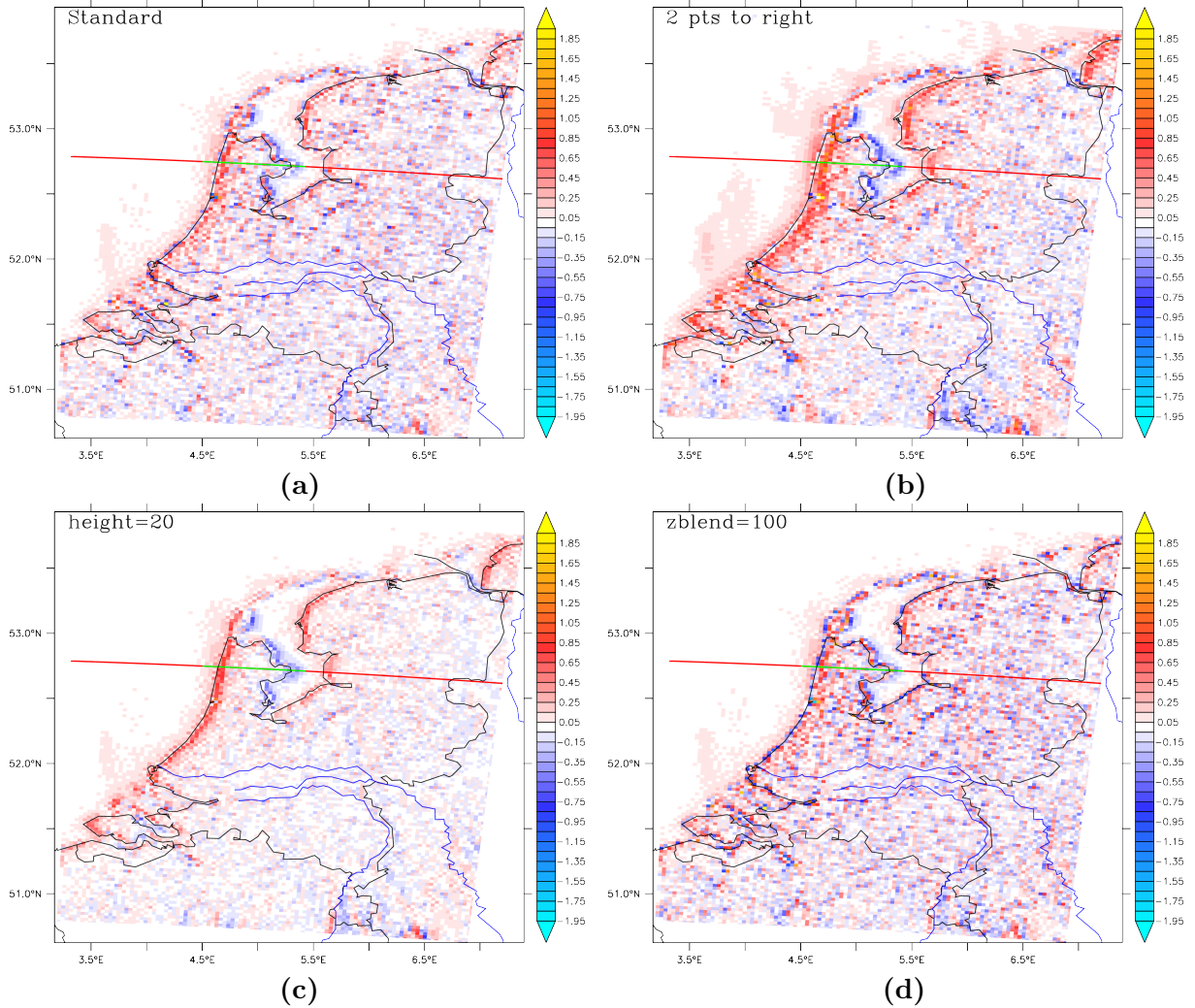


**Figure 7:** Difference between the transformed wind speed  $\hat{U}_{\text{ref}}$  according to eq. (15) and the modelled wind speed for the standard value  $z_{\text{obs}} = z_{\text{ref}} = 10$  m. Monthly-means for January 2012 are shown. **a)** as in (15), **b)** transformation occurs over two grid points, i.e.  $i + 1 \rightarrow i + 2$  in (15), **c)** using  $z_{\text{obs}} = z_{\text{ref}} = 20$  m instead of the standard 10 m, **d)** using a blending height of 100 m. In Sect. 4.3 vertical sections are evaluated along the transect shown by red and green lines.

partly land and partly water, we repeat the calculation for a transformation over two grid points (i.e., using  $i + 2$  instead of  $i + 1$  in (15)). Figure 7b shows that the same over/underestimation is obtained.

In Sect. 3.3 we saw that the 10 m wind is higher than suggested by an extrapolation of the logarithmic profile obtained from wind speeds at greater height. To see whether this deviation causes the discrepancies seen in Fig. 7a, we repeat the calculation using  $z_{\text{obs}} = z_{\text{ref}} = 20$  m instead of 10 m. The result is depicted in Fig. 7c and shows a large-scale pattern of over- and underestimation of the wind speed as before. However, the pattern is much smoother, and the differences over land are much smaller. Obviously, the use of the ten-metre wind introduces a lot of noise (small-scale variability), presumably because it is too much determined by the local roughness (see also discussion in Sect. 3.3). Nevertheless, the open water wind is underestimated.

A central assumption in the transformation process is that the wind at the blending height of 60 m is spatially constant, i.e., independent of the local roughness. To test whether other choices for the blending height yield better results, we repeat the calculation for different values of the

blending height. As an example, the result for  $z_{\text{blend}} = 100$  m is shown in Fig. 7d. Although the differences are slightly smaller along the coast, the two Figures (7a and d), are very similar, and other choices of  $z_{\text{blend}}$  do not give better results (not shown). The choice of the blending height is not crucial for the results of the BHM.

The logarithmic wind profile (1) and therefore all calculations in Sect. 2, and especially eq. (9), are only valid if the atmosphere is neutrally stratified. In (un)stable cases deviations from the logarithmic profile occur. To avoid such cases we repeated the calculation for cases with high wind speeds ( $> 10$  m/s over land). The result is an even larger bias along the coasts (not shown).

It appears that the transformation (15) is not suited to derive the open-water wind from nearby wind measurements on land. It leads to an underestimation of the wind over water by  $\approx 0.5$  m/s.

## 4.2 Transformation over larger distances

Often there are no measurements available from nearby land points, and measurements from station relatively far away from the water body in question have to be used. From the results in Sect. 4.1 we expect that this will lead to even worse results. As an example, we take the modelled wind at Schiphol and transform it to all other grid points using the local roughness at that point. Figure 8 confirms our expectation. The procedure results in a severe underestimation ( $\lesssim 1$  m/s) of the wind over large open water bodies (Lake IJssel, Rhine-Meuse delta), and an overestimation over land that increases with distance from the coast.

Figure 8 is for January, when westerly wind directions are predominant. Not surprisingly, the panels for all wind directions (upper left) and for westerly wind only (upper right) look very similar. However, the patterns also do not change much when other wind directions are considered (lower row). In all cases the application of the BHM leads to an underestimation of winds over water, and an overestimation of winds over land. This pattern is only modified near the coast. Obviously, the influence of the sea reaches further inland than anticipated by the BHM. Note in this context that the wind speed is usually low when the wind comes from land (East or South). Both wind speed and wind directions can be quite different at the coast in the north of the Netherlands than they are at Schiphol.

Instead of looking at the difference between the modelled and the transformed wind speeds as in Fig. 8, it is instructive to have a look at their normalized root mean square difference (NRMSD),  $100 \cdot \frac{\sqrt{\langle (\hat{U}_{10} - \hat{U}_{10})^2 \rangle}}{\langle \hat{U}_{10} \rangle}$ , where  $\langle \dots \rangle$  denotes the time average. It measures the discrepancy between the two variables, irrespective of its sign, relative to the mean wind speed. Figure 9 shows how the discrepancy between the extrapolated and the modelled wind rapidly increases with distance from Schiphol, and that it sharply increases over water. In fact, the discrepancy is larger over Lake IJssel than over land at the east side of the lake, even though the distance to Schiphol is larger there. The increase of the NRMSD with distance from Schiphol reflects the fact that wind systems have a final size. Different regions can be influenced by different systems. It is a real effect that is neglected in the BHM.

## 4.3 Reasons for failure

### 4.3.1 Blending height

As we have shown, deriving an open water wind speed using (9) does not yield satisfactory results. The central assumption of the BHM is the existence of a blending height where the wind is independent of the local roughness. We now investigate this assumption.

Figure 10 shows different cross sections of wind speed along the transect in Fig. 7a. From the figure it is obvious that the wind speed changes rather abruptly across the land-sea boundary at all heights. Within the chosen 0.25 m/s intervals there are hardly any adjacent grid points with

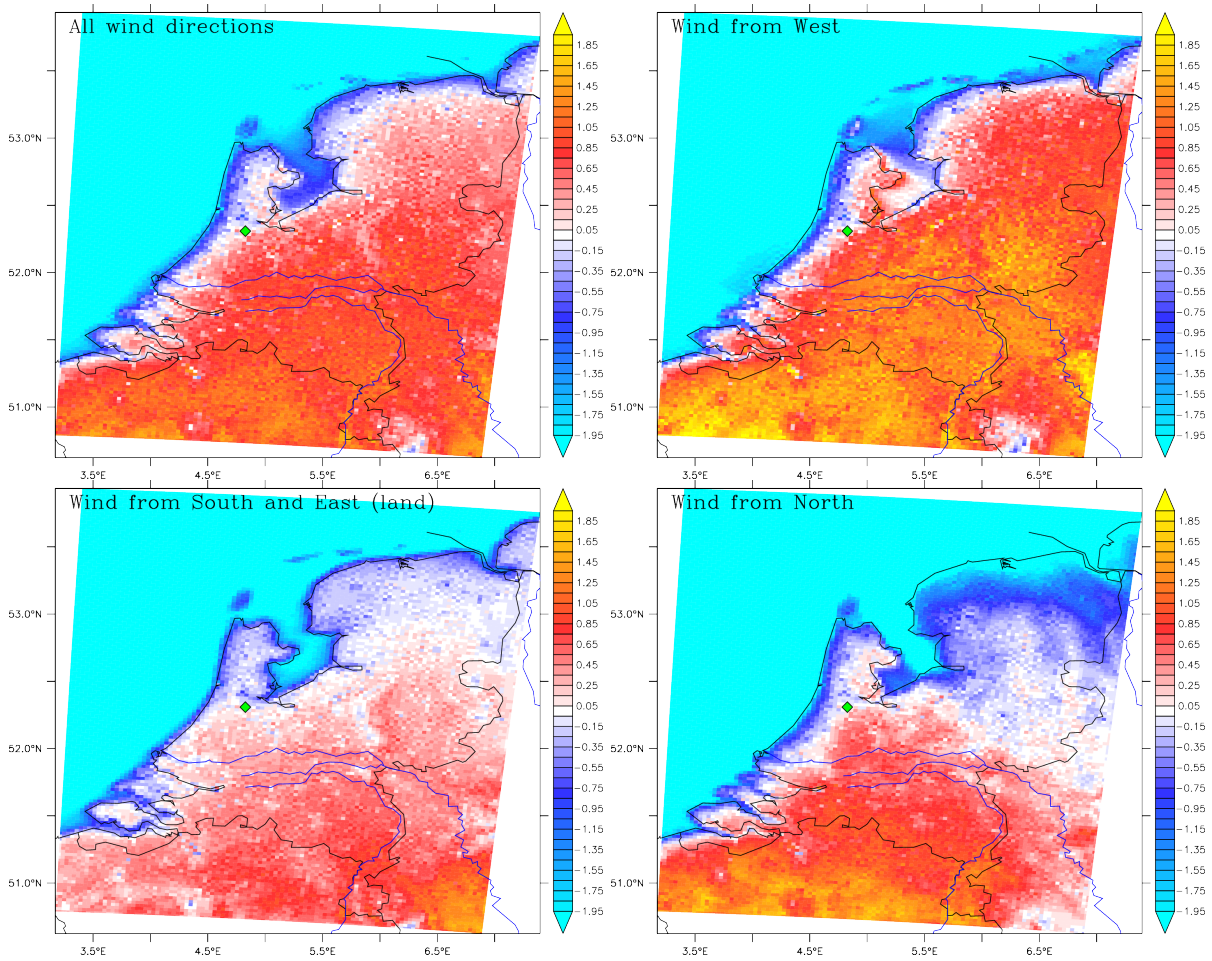


**Figure 8:** As Figure 7a, but with the input wind taken from Schiphol (green diamond) and the local roughness at each grid point to calculate  $\hat{U}_{10}$ . In other words, at each grid point  $\hat{U}_{10}$  is calculated from the wind at Schiphol and the local roughness. The different panels are for different wind directions at Schiphol as indicated (West - between SW and NW, land - between NE and SW, North - between NW and NE).

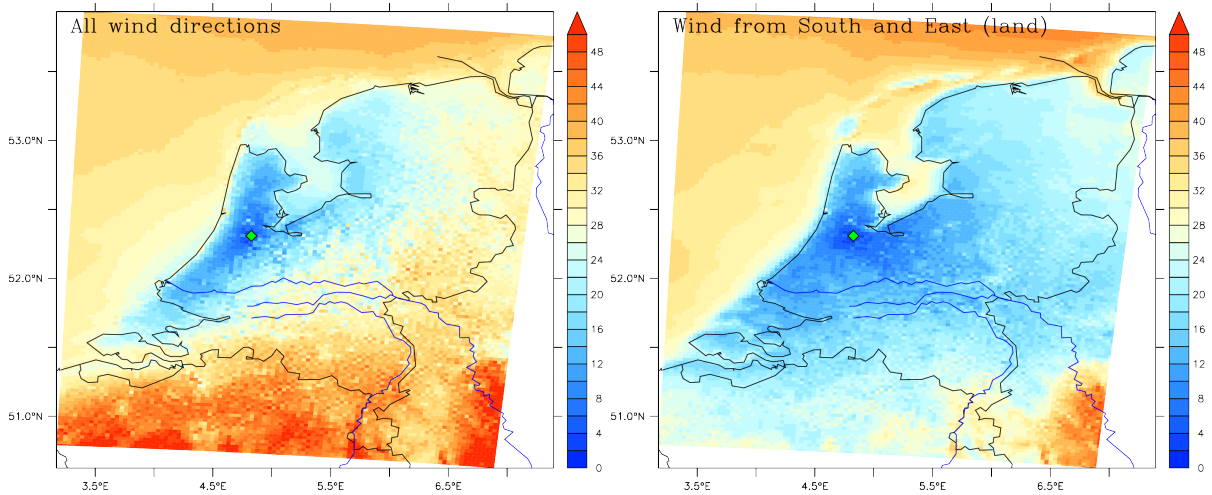


**Figure 9:** As Figure 8, but for the normalized root mean square difference, for all wind directions (left) and winds from land only (right).

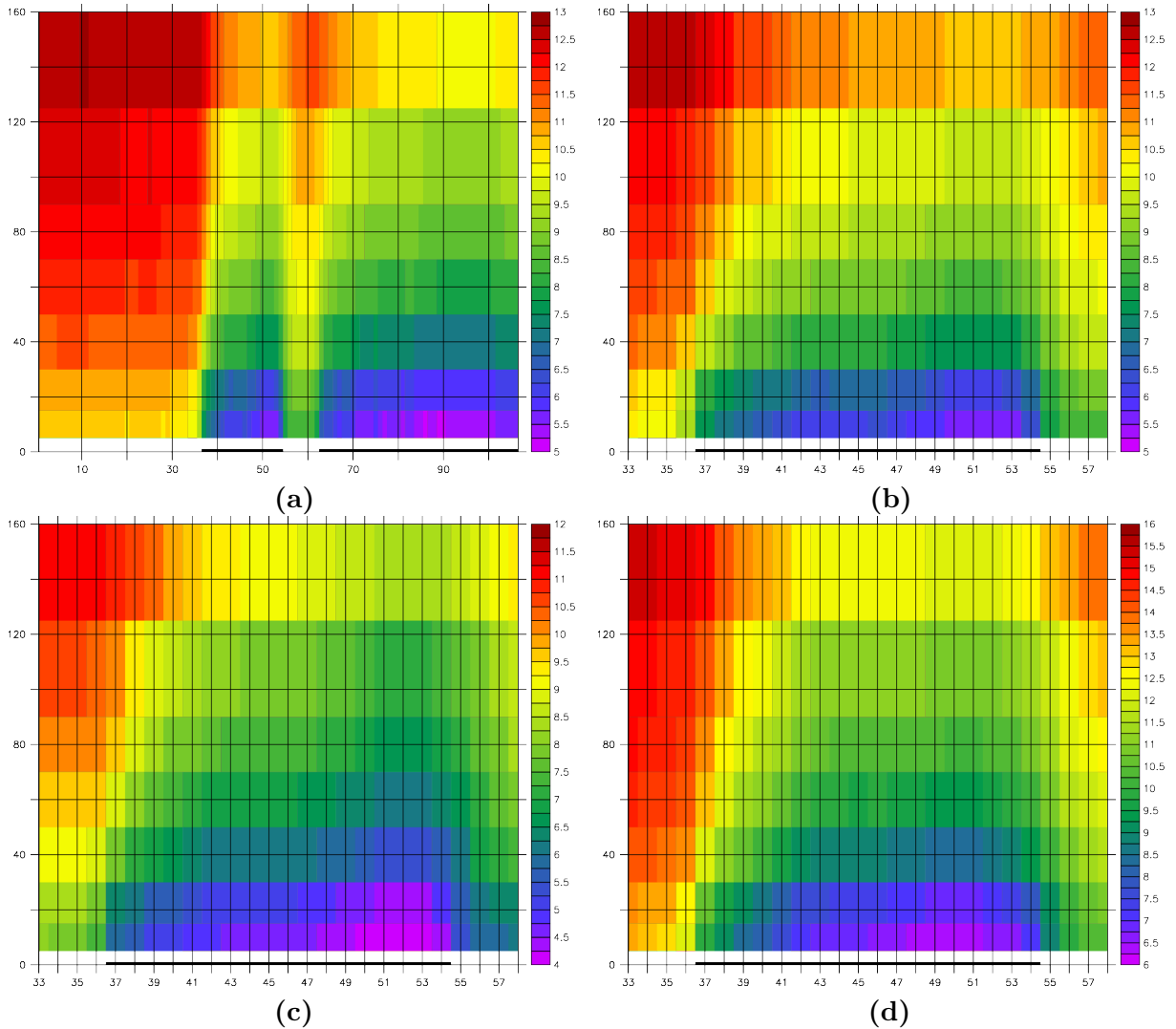


**Figure 10:** Vertical cross sections of wind speed (Jan. 2012) in the lower 160 m of the atmosphere. **a)** Monthly mean along the whole transect shown in Fig. 7. **b)** Monthly mean along the green part of the transect. **c)** A low wind case (11 Jan. 2012, 12:00 UTC), and **d)** a high wind case (12 Jan. 2012, 18:00 UTC) along the green part of the transect. Note the different colour scales in c) and d). The black line at the bottom of each panel denotes land points. The x-values denote the positions of the grid points, so that the grid boxes straddle the vertical grid lines.

the same wind speed. Due to the predominantly westerly winds, the region with the maximum wind speed change moves eastward with height. The wind at height needs some time to “feel” the changing surface characteristics. The abrupt change in wind speed occurs for the monthly-mean values (Fig. 10a,b) as well as for low and high instantaneous wind speeds (c,d). It is obvious that the concept of a blending height at which the wind is constant across, and not influenced by, the land-water boundary does not make sense.

It is instructive to note that Bottema (2007) anticipated this result by applying the simple theory of Wood (1982). For the development of the height of the internal boundary layer  $h_{IBL}$  behind a step change in surface roughness (e.g., land  $\rightarrow$  water, or *vice versa*), Wood (1982) finds

$$h_{IBL}(x) = 0.28 z_{0,r} \left( \frac{x}{z_{0,r}} \right)^{0.8}, \quad (16)$$

where  $z_{0,r}$  is the roughness length of the downstream surface, and  $x$  is the downstream distance

from the jump. The values for surface roughness for North Holland (land area to the west of Lake IJssel) as used in the model range between 0.05 m and 0.5 m. Inserting these two values into (16) shows that the height of the internal boundary layer reaches 60 m within respectively  $\approx 1.8$  km and  $\approx 1$  km (see also Fig. 4 in Van den Brink et al., 2017). In other words, the impact of a sudden roughness change is felt at the blending height well within one grid cell of HARMONIE, confirming the results shown in Figures 1 and 10. Consequently, the wind speed will be affected, although eq. (16) does not tell us how. The underlying assumption of the BHM is that the wind at the blending height is undisturbed over a distance that is representative for the bulk of the water surface. This assumption is clearly not valid.

### 4.3.2 Macro wind

As shown in Sect. 2.5, the BHM is a simplification of the complete WR2LM. We now investigate whether the encountered problems result from the simplification, or whether they are inherent to the WR2LM. To extrapolate winds measured over land to winds over water, the BHM as applied by RWS assumes that the wind at the blending height of 60 m is constant across the land-water boundary. We have shown that this assumption is not valid. The equivalent assumption in the WR2LM is that the macro wind  $S_h$  at the top of the Ekman layer is constant across the boundary. We now test the validity of this assumption in the HARMONIE output. To calculate  $S_h$ , we need to know the meso roughness  $z_{0,m}$ . From the meso roughness we can calculate  $u_{*,m}$  using (11), and subsequently  $S_h$  using (12a) and (14).

The roughness in the model is representative for the grid size of roughly 2.5 km, which is larger than the few hundred metres assumed in the WR2LM to determine the local roughness. This makes the distinction between a local and a meso roughness somewhat questionable. Our first choice is therefore to take the two equal and have  $z_{0,m} = z_0$ . According to Wieringa and Rijkoort (1983), the meso roughness should be representative for an upstream area of 5 km  $\times$  5 km. With predominantly westerly winds, upstream is to the west of the grid point we consider. The second (third) choice for  $z_{0,m}$  is therefore the mean over five (ten) kilometres to the west, corresponding to two (four) grid boxes. An average over 5 km corresponds to the recommendation of Wieringa and Rijkoort (1983), while averaging over a larger distance tests whether an average over a larger area would improve the results. In all cases the average is determined by averaging the logarithm of the surface roughness (Bottema and Klaassen, 1998). Finally, as theoretically  $U_{\text{bld}} = U(z_{\text{bld}})$ , we can also use the modelled wind at  $z_{\text{bld}}$  instead of  $U_{\text{bld}}$  in (11) to calculate  $u_{*,m}$ , and from that the meso wind.

Figure 11 shows the macro wind speed  $S_h$  over the region of Lake IJssel at one particular time step (20 January 2012, 00:00 UTC), calculated from four different combinations of the choices for  $z_{0,m}$  and  $U_{\text{bld}}$ . Obviously, the macro wind is not constant across land-water boundaries for any of the choices made. So the basic assumption behind using the WR2LM to extrapolate across a land-water boundary is not backed by the HARMONIE output.

According to the WR2LM, the macro wind speed  $S_h$  equals the wind speed  $U_{\text{ek}} = U(z = h_{\text{ek}})$  at the height of the Ekman layer. To investigate this assumption further, Fig. 12 displays the height of the Ekman layer  $h_{\text{ek}}$  according to (13), the macro wind speed  $S_h$  according to (14), the wind speed at the height of the Ekman layer  $U_{\text{ek}}$ , and a vertical cross section of the wind speed along the black line in Fig. 12c, all averaged for January 2012. For the meso roughness the logarithmic average of the roughness over 5 km to the west of the point considered is taken, but other choices give similar results.

The height of the Ekman layer (Fig. 12a and d) strongly reflects the surface roughness (not shown) and varies between 400 m over water to more than 1 km over rough land, e.g., over the urbanized areas in the west of the Netherlands. The transition from low to high values is rather abrupt, reaching several hundred metres within a few grid points (Fig. 12d). The macro wind speed (Fig. 12b) follows the pattern of the Ekman layer height. It is clearly not constant

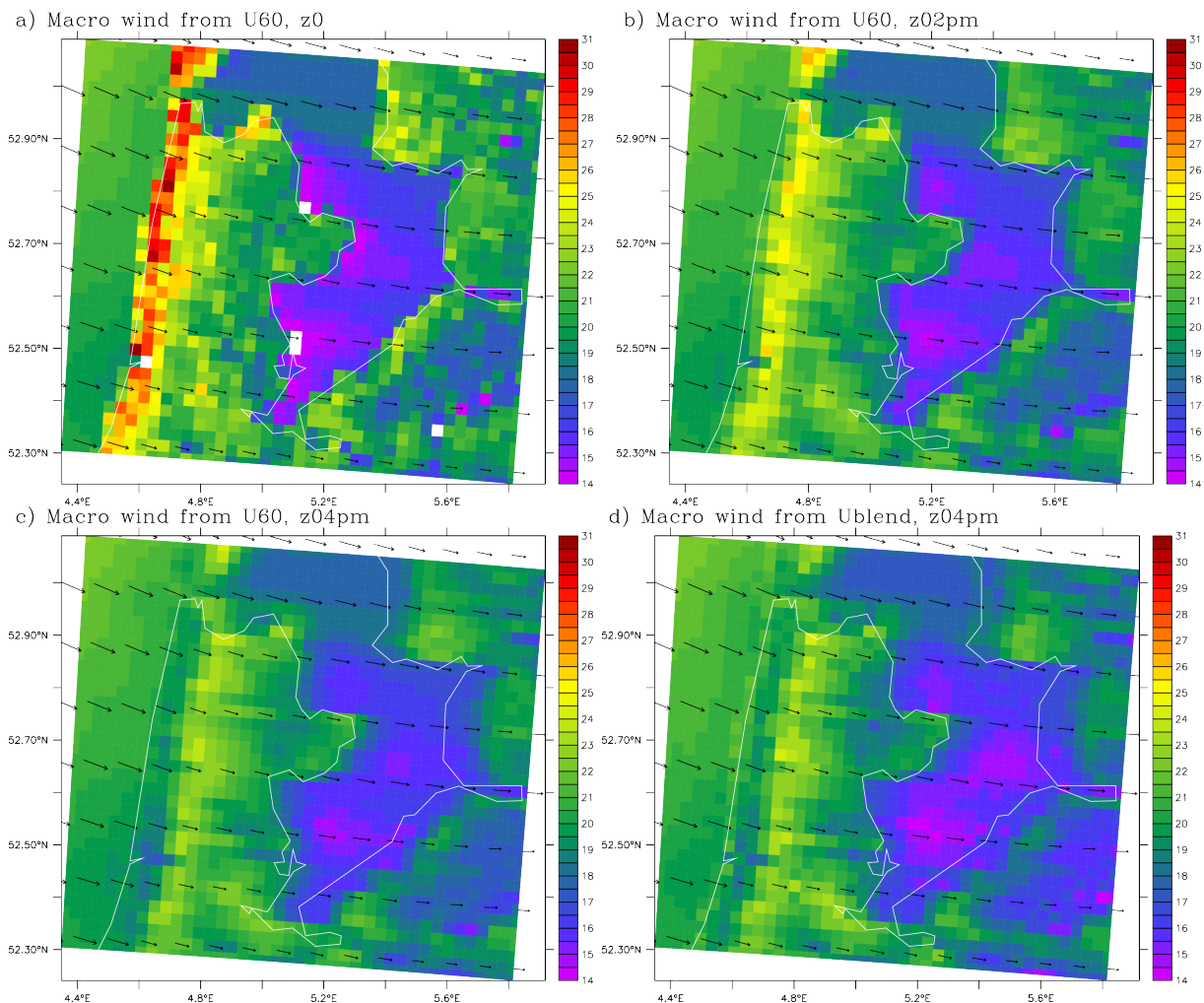


**Figure 11:** Macro wind on 20 January 2012, 00:00 UTC, in the region of Lake IJssel according to different choices for  $z_{0,m}$  (colours), and the wind (direction) at the blending height (arrows). **a)**  $z_{0,m} = z_0$  and  $U_{\text{bld}} = U(z_{\text{bld}})$ ; **b)** roughness averaged over two grid boxes and  $U_{\text{bld}} = U(z_{\text{bld}})$ ; **c)** roughness averaged over four grid boxes and  $U_{\text{bld}} = U(z_{\text{bld}})$ ; **d)** roughness averaged over four grid boxes and  $U_{\text{bld}}$  derived from local roughness (i.e., eq. (7a)).

across land-water boundaries (see also Fig. 11), but exhibits rather steep jumps that reach 4 m/s within two grid points in the southern part of Lake IJssel.

The wind at the Ekman height (Fig. 12c) is much smoother than the macro wind, suggesting that the WR2LM overestimates the impact of surface roughness on the wind at height. However, a step change at land-water boundaries is still visible. This result is confirmed by Fig. 12d. A comparison between panels b) and c) of Fig. 12 immediately shows (see Fig. 13) that the macro wind  $S_h$  does not equal the wind at the height of the Ekman layer, i.e.,

$$S_h \neq U(z = h_{\text{ek}}). \quad (17)$$

Equality of these two winds is a central assumption of the WR2LM. From the results shown in Figs. 12 and 13 we must conclude that the WR2LM is based on an invalid assumption. This conclusion is further backed by the cross-section in Fig. 12d. Both the height of the Ekman layer and the isotachs (lines of equal wind speed) clearly follow the surface roughness, but they do not vary in parallel, demonstrating that the wind speed at the height of the Ekman layer is not constant across land-sea boundaries.

The plots in Figure 12 look qualitatively similar (not shown) if we

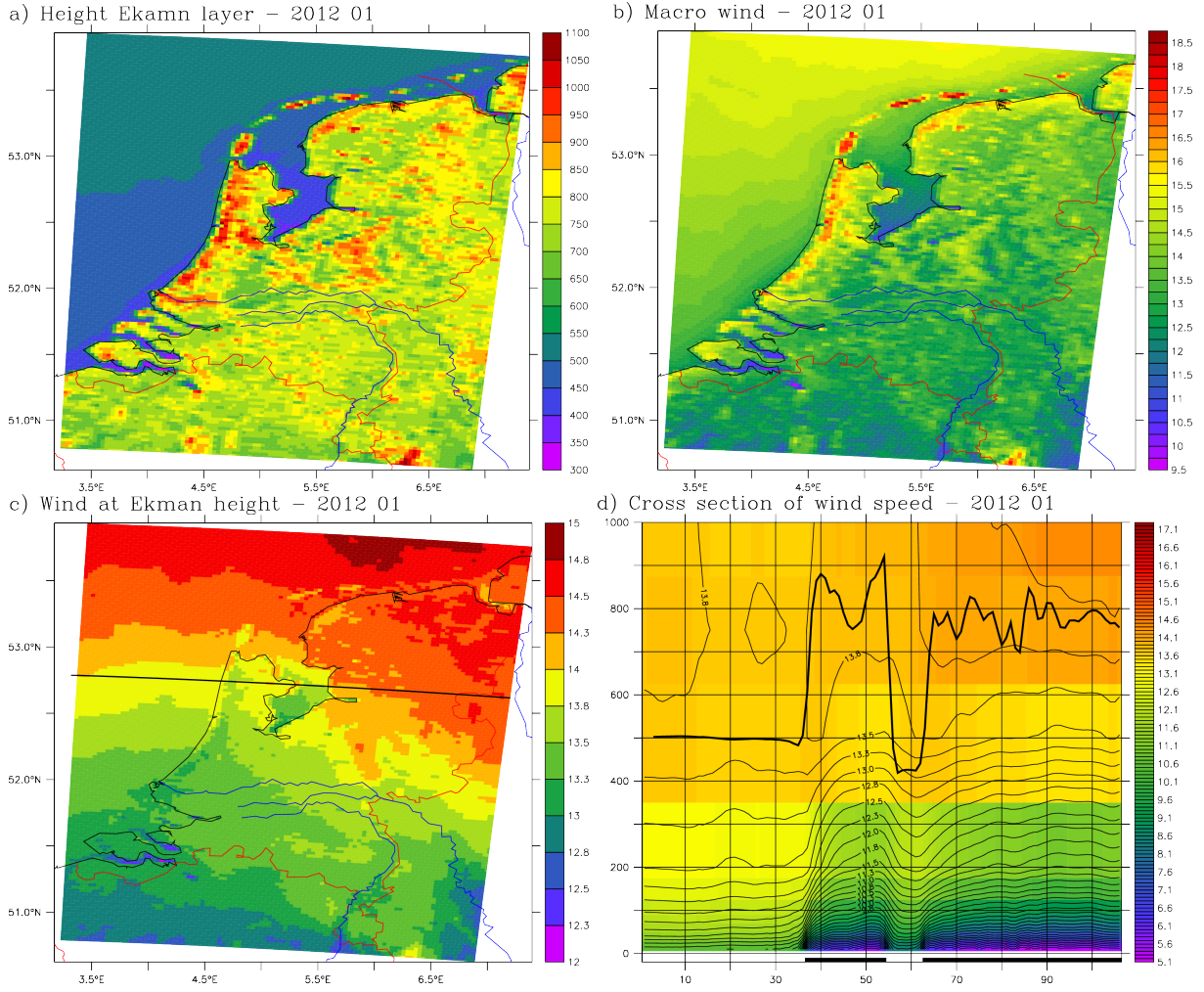


**Figure 12:** **a)** Height of the Ekman layer according to (13), using the logarithmic average over 5 km to the west of the point considered as the meso roughness  $z_{0,m}$ ; **b)** macro wind speed  $S_h$  according to (14), **c)** wind speed at the height of the Ekman layer, and **d)** vertical cross section of wind speed along the black line in c), where the colours are non-interpolated values and the contour lines represent an interpolated field. The thick black line denotes the height of the Ekman layer ( $h_{ek}$ ). The black line at the bottom indicates land points in the model. All panels display monthly means over January 2012.

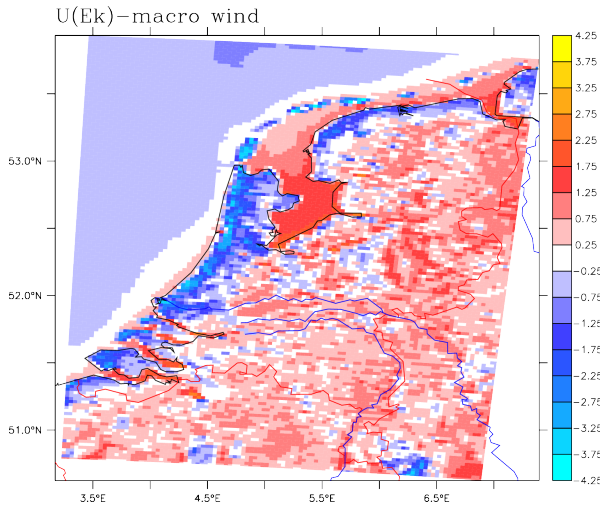


**Figure 13:** Difference between the wind at the height of the Ekman layer ( $U_{ek}$ ) and the macro wind ( $S_h$ ) for January 2012. It is actually the difference between panels c) and b) of Fig. 12.

- look at instantaneous values instead of monthly means,
- select situations in which the wind direction is *not* west,
- select only cases with high wind speed (less impact of stability),
- take a summer month,
- change the height of the calculated Ekman layer by changing the value of  $A$ ,
- determine  $z_{0m}$  by averaging  $z_0$  over much larger upstream distances,
- use other values for the blending height.

Together this shows that the WR2LM does not agree with the output of HARMONIE. In particular, the wind at land-water boundaries does not change as described by the two-layer model. Therefore, it should not be used to infer the wind over open water from wind measured at land stations. Obviously, this conclusion also holds for the BHM, as this model is a simplification of the WR2LM.

## 5 Discussion

Using output from the HARMONIE model we have shown that the wind over water cannot be derived from observations over land by applying the BHM or the WR2LM. We now look a bit deeper into the background of the WR2LM and show that it was *not* intended to extrapolate across land-sea boundaries or over large distances, but to *interpolate* between adjacent points. As the BHM is a simplification of the WR2LM, this restriction carries over to the former.

### 5.1 The theory behind the WR2LM

The basic theory behind the WR2LM is described in detail in Blackadar and Tennekes (1968) and summarized in Tennekes (1973). In these papers equations (12a) and (12b) are obtained by dividing the planetary boundary layer into an inner and an outer layer. For both layers asymptotic solutions of the governing flow equations are found and matched across a height range in which both of them must be valid simultaneously. While this resembles the idea of a blending height where the velocity can be equally well described by the small-scale (local) and the large-scale (meso) roughness, their matching height does not have a fixed value, but depends on surface roughness and friction velocity. Formally, the matching height is where simultaneously  $z \gg z_0$  (far away from the surface) and  $z \ll h_{ek}$  (far below the Ekman height). As  $z_0$  changes by at least two orders of magnitude between land and water, the matching height will also change considerably. There is no universal value for the height of the transition region or its surrogate, the blending height.

### 5.2 The WR2LM

Wieringa and Rijkoort (1983) developed their model to *interpolate* between wind stations, not to *extrapolate* into regions with no measurements. The macro wind is calculated from the measured station values of  $U_{10}$  and interpolated to the desired position, where it is translated back to the local near-surface wind. The smoothness of the macro wind field (Fig. 4.7 of Wieringa and Rijkoort (1983), or our Fig. 12c) ensures the feasibility of this approach, and Stepek and Wijnant (2011) validated it by comparing near-surface winds interpolated to a measurement station with the observed values at that station.

However, Wieringa and Rijkoort (1983) caution against using their model across land-sea boundaries. On page 81 of their report they write<sup>3</sup>:

De toepassing van de gebruikte similariteitsformules vereist formeel een homogene planetaire grenslaag met neutrale stabiliteit. De homogeniteit heeft zowel betrekking op het terrein als op de horizontale luchtdrukgradiënt. Dit laatste impliceert dat belangrijke horizontale temperatuurgradiënten niet toelaatbaar zijn, omdat deze aanleiding geven tot extra drukgradiënten (zogenaamde „barokliniciteit”). De methodiek zal dus op de kustlijn niet toepasbaar zijn, zowel vanwege de grote verandering in terreintype als vanwege de mogelijkheid van grote temperatuurverschillen tussen land en zee. Boven een  $5 \times 5 \text{ km}^2$  blok te land, gekarakteriseerd door de plaatselijke mesoruwheid  $z_{om}$ , mogen we deze homogeniteit wél veronderstellen.

Although Wieringa and Rijkoort (1983) refer to the land-sea transition, their argument is also applicable to transitions between land and lakes. Here, too, the roughness changes dramatically, and temperature gradients can be large, especially in the case of the larger water bodies. Consequently, Wieringa and Rijkoort (1983) do not use coastal stations to derive their wind climatology, and they do not interpolate over large inland water bodies!

Finally, it should be mentioned that Wieringa and Rijkoort (1983) do not give a theoretical argument for the use of 60 m as the blending height or the boundary between the lower and the upper layer. The choice is based on the observation that below roughly 60 m the magnitude of the wind changes, while the direction is roughly constant, whereas above that height the speed hardly changes, but the direction does (p 36). On page 53 they state that “De hoogte van die oppervlaktelaag bedraagt in een onstabiele of neutrale grenslaag ongeveer 60 tot 100 m, afhankelijk van de terreinruwheid” (In an unstable or neutral boundary layer, the height of that surface layer amounts to approximately 60 to 100 m, depending on the surface roughness.) Using a simple model of the boundary layer, Beljaars (1987) arrives at a lower estimate of 17–40 m for the blending height. So 60 m appears to be less of an cast-iron value as it is often assumed to be. Note, however, that using a different value for the blending height still leads to discrepancies between the HARMONIE output and the transformed winds (Sect. 4.1).

### 5.3 The curvature problem

It has long been known that application of the potential wind concept (7c) leads to the *curvature problem*, where maximum winds seem to increase *inland*, away from the coast. This problem is discussed at great length by Caires et al. (2012). They identify a lot of factors unaccounted for in the application of the potential wind concept and conclude that it is not feasible to incorporate all of them into the concept. Most importantly, they question the assumptions of neutral stability and the wind speed at the blending height being unaffected by the surface roughness changes. In this report we have shown that the latter assumption is indeed not valid. Instead of using the potential wind concept, Caires et al. (2012) advise to use numerical weather models to transform measured winds from land to water.

## 6 Summary and conclusion

Routine wind measurements are usually taken on land. To obtain information over the wind over water (e.g., inland lakes), RWS transforms the measured wind from land to water, assuming

---

<sup>3</sup>My translation: Formally, the application of the similarity equations requires a homogeneous planetary boundary layer with neutral stability. The homogeneity applies both to the terrain and the horizontal pressure gradient. The latter implies that substantial horizontal temperature gradients are not allowed, because they give rise to extra pressure gradients (so-called “baroclinicity”). Therefore the method is not applicable on the coastline, both because of the large change in the type of the terrain, and because of the possibility of large temperature differences between land and sea. However, above a  $5 \times 5 \text{ km}^2$  area of land, characterized by the local meso roughness  $z_{om}$ , this homogeneity may be assumed.

a logarithmic wind profile and the existence of a well-defined height at which the wind is independent of the (local) surface roughness. In the simplest form of the theory (BHM) this height is taken to be the constant blending height of 60 m, in the more involved form (WR2LM) it is the varying height of the Ekman layer. Due to the sparseness of wind observations at height, it is hard to validate these assumptions with observations. It should be noted, however, that the WR2LM was not intended to extrapolate across land-water boundaries.

Instead of using observations, we here use the output of a high-resolution numerical weather model to test the theory. A comparison of the model output with observations at two sites (one on land, one at sea) that provide wind profiles suggests that the model is suited to test the theory. While modelled and observed wind speeds are nearly identical at the land site, the modelled winds exceed the measured ones by roughly 10% at the sea site. However, at both sites the shapes of the modelled and observed wind profiles correspond very well. It turns out that the wind is not sufficiently constant neither at the blending height nor at the height of the Ekman layer to allow extrapolation across the land-water boundary. Consequently, the transformed 10 m winds differ from the respective model winds.

In short, the transformation currently used by RWS does not give reliable results and should not be used. Like Caires et al. (2012) we recommend that a well-calibrated and evaluated atmosphere model is used instead. Ideally, several models should be intercompared and validated against observation to identify the best one to use. However, running high-resolution atmosphere models is expensive and time-consuming, and a thorough intercomparison of several models is probably not feasible. As HARMONIE is used extensively at KNMI and has proven to give good results in general, this model should be used as the starting point and its quality in terms of wind over water, in particular small inland water bodies, should be determined. Only if this exercise reveals a bad performance of HARMONIE, other models should be investigated.

## References

- Baas, P. (2014): Final Report of WP1 of the WTI2017-HB Wind Modelling project. *Scientific Report*, WR-2014-2, KNMI, De Bilt, <http://bibliotheek.knmi.nl/knmipubWR/WR2014-02.pdf>
- Baas, P., and H. de Waal (2012): Interim report on the validation of Harmonie. [https://cdn.knmi.nl/system/data\\_center\\_publications/files/000/069/154/original/1204199004hye0004v2rinterimreportonthevalidationofharmonie1.pdf](https://cdn.knmi.nl/system/data_center_publications/files/000/069/154/original/1204199004hye0004v2rinterimreportonthevalidationofharmonie1.pdf)
- Beljaars, A.C.M. (1987): On the memory of wind standard deviation for upstream roughness. *Boundary-Layer Meteorol* **38**, 95-101, doi: 10.1007/BF00121557
- Bengtsson, L., U. Andrae, T. Aspeli, Y. Batrak, J. Calvo, W. de Rooy, E. Gleeson, B. Hansen-Sass, M. Homleid, M. Hortal, K. Ivarsson, G. Lenderink, S. Niemelä, K.P. Nielsen, J. Onvlee, L. Rontu, P. Samuelsson, D.S. Muñoz, A. Subias, S. Tijn, V. Toll, X. Yang, and M.Ø. Körtzow (2017): The HARMONIE-AROME Model Configuration in the ALADIN-HIRLAM NWP System. *Mon. Wea. Rev.*, **145**, 1919-1935, doi: 10.1175/MWR-D-16-0417.1
- Blackadar, A.K., and H. Tennekes (1968): Asymptotic similarity in neutral barotropic planetary boundary layers. *J. Atm. Sci.*, **25**, 1015-1020
- Bottema, M., and W. Klaassen (1998): Landscape roughness parameters for Sherwood Forest – Validation of aggregation models. *Boundary-Layer Meteorology*, **89**, 317–347.
- Bottema, M. (2007): Measured wind-wave climatology Lake IJssel (NL): Main results for the period 1997–2006. Rijkswaterstaat RIZA (Lelystad NL), Report 2007.020, ISBN: 978-90-369-1399-7; <http://publicaties.minienm.nl/documenten/measured-wind-wave-climatology-lake-ijssel-nl-main-results-for-t>
- Caires, S., H. de Waal, J. Groeneweg, G. Groen, N. Wever, C. Geerse, and M. Bottema (2012): Assessing the uncertainties of using land-based wind observations for determining extreme open-water winds. *J. Wind Eng. Ind. Aerodyn.*, **110**, 70-85, doi: 10.1016/j.jweia.2012.07.009
- Dee, D.P., S.M. Uppala, A.J. Simmons, P. Berrisford, P. Poli, S. Kobayashi, U. Andrae, M.A. Balmaseda, G. Balsamo, P. Bauer, P. Bechtold, A.C.M. Beljaars, L. van de Berg, J. Bidlot, N. Bormann, C. Delsol, R. Dragani, M. Fuentes, A.J. Geer, L. Haimberger, S.B. Healy, H. Hersbach, E.V. Hólm, L. Isaksen, P.

- Källberg, M. Köhler, M. Matricardi, A.P. McNally, B.M. Monge-Sanz, J.-J. Morcrette, B.-K. Park, C. Peubey, P. de Rosnay, C. Tavalato, J.-N. Thépaut, and F. Vitart (2011): The ERA-Interim reanalysis: configuration and performance of the data assimilation system. *Q.J.R. Meteorol. Soc.*, **137**, 553-597, doi: 10.1002/qj.828
- De Rooy, W., and H. de Vries (2017): Harmonie verification and evaluation. *HIRLAM Tech. Rep.* **70**, 79 pp. [http://hirlam.org/index.php/publications-54/hirlam-technical-reports-a/doc\\_download/1805-hirlam-technicalreport-70](http://hirlam.org/index.php/publications-54/hirlam-technical-reports-a/doc_download/1805-hirlam-technicalreport-70)
- Geertsema, G.T., and H.W. an den Brink (2014): Windkaart van Nederland op 100 meter hoogte (in Dutch). *Technical Report*, TR-351, KNMI, De Bilt, <http://bibliotheek.knmi.nl/knmipubTR/TR351.pdf>
- Kalverla, P.C., G.-J. Steeneveld, R.J. Ronda, and A.A.M. Holtslag (2017): An observational climatology of anomalous wind events at offshore meteor mast IJmuiden (North Sea). *J. Wnd. Eng. Ind. Aerodyn.*, **165**, 86-99, doi: 10.1016/j.jweia.2017.03.008
- Lenderink, G., and A.A.M. Holtslag (2004): An updated length-scale formulation for turbulent mixing in clear and cloudy boundary layers. *Quart. J. Roy. Meteor. Soc.*, **130**, 3405-3427, doi: 10.1256/qj.03.117
- Masson, V., P. Le Moigne, E. Martin, S. Faroux, A. Alias, R. Alkama, S. Belamari, A. Barbu, A. Boone1, F. Bouyssel, P. Brousseau, E. Brun, J.-C. Calvet, D. Carrer, B. Decharme, C. Delire, S. Donier, K. Essauouini, A.-L. Gibelin, H. Giordani, F. Habets, M. Jidane, G. Kerdraon, E. Kourzeneva, M. Lafaysse, S. Lafont, C. Lebeaupin Brossier, A. Lemonsu, J.-F. Mahfouf, P. Marguinaud, M. Mokhtari, S. Morin, G. Pigeon, R. Salgado, Y. Seity, F. Taillefer, G. Tanguy, P. Tulet, B. Vincendon, V. Vionnet, and A. Voldoire (2013): The SURFEXv7.2 land and ocean surface platform for coupled or offline simulation of earth surface variables and fluxes. *Geosci. Model Dev.*, **6**, 929-960, doi: 10.5194/gmd-6-929-2013
- Tennekes, H. (1973): The logarithmic wind profile. *J. Atmos. Sci.*, **30**, 234-238
- Stepek, A., and I.L. Wijnant (2011): Interpolating wind speed normals from the sparse Dutch network to a high resolution grid using local roughness from land use maps. *Technical Report*, TR-321, KNMI, De Bilt, <http://bibliotheek.knmi.nl/knmipubTR/TR321.pdf>
- Sterl, A. (2017): Drag at high wind velocities - a review. *Technical Report*, TR-361, KNMI, De Bilt, <http://bibliotheek.knmi.nl/knmipubTR/TR361.pdf>
- Sterl, A. (2018): Brief review of wind and drag transformations in WBI2017. *Technical Report*, TR-363, KNMI, De Bilt, <http://bibliotheek.knmi.nl/knmipubTR/TR363.pdf>
- Van Nieuwkoop, J., P. Baas, S. Caires, and J. Groeneweg (2015): On the consistency of the drag between air and water in meteorological, hydrodynamic and wave models. *Ocean Dynam.* **65**, 989-1000, doi: 10.1007/s10236-015-0849-3
- Van den Brink, H., P. Baas, and G. Burgers (2013): Towards an approved model set-up for HARMONIE. *Contribution to WP 1 of the SBW-HB Wind modelling project*, Royal Netherlands Meteorological Institute (KNMI), [https://cdn.knmi.nl/system/data\\_center\\_publications/files/000/069/397/original/towards\\_an\\_approved\\_model\\_setup\\_for\\_harmonie\\_sbw\\_milestone1\\_final.pdf](https://cdn.knmi.nl/system/data_center_publications/files/000/069/397/original/towards_an_approved_model_setup_for_harmonie_sbw_milestone1_final.pdf)
- Van den Brink, H.W., I.L. Wijnant, F.C. Bosveld en A. Stepek (2017): Klimatologie van extreme windvlagen (In Dutch). *Scientific Report*, WR-2017-01, KNMI, De Bilt, <http://bibliotheek.knmi.nl/knmipubWR/WR2017-01.pdf>
- Verkaik, J.W. (2006): On Wind and Roughness over Land. *Ph.D. Thesis, Wageningen University, The Netherlands*, 123p, <http://edepot.wur.nl/121786>
- Verkaik, J.W., A.A.M. Holtslag (2007): Wind profiles, momentum fluxes and roughness lengths at Cabauw revisited. *Boundary-Layer Meteorology* **122**, 701-719, doi: 10.1007/s10546-006-9121-1 (also chap. 3 of Verkaik (2006))
- Wieringa, J. (1986): Roughness-dependent geographical interpolation of surface wind speed averages. *Q. J. R. Meteorol. Soc.*, **112**, 867-889
- Wieringa, J., and P.J. Rijkoort (1983): Windklimaat van Nederland (In Dutch). Staatsdrukkerij, 's Gravenhage (NL)
- Wood, D.H. (1982): Internal boundary layer growth following a step change in surface roughness. *Boundary-Layer Meteorol.* **22**, 241-244, doi: 10.1007/BF00118257
- Wu, J. (1982): Wind-stress coefficients over sea surface from breeze to hurricane. *J. Geophys. Res.*, **C87**, 9704-9706, doi: 10.1029/JC087iC12p09704



**Royal Netherlands Meteorological Institute**

PO Box 201 | NL-3730 AE De Bilt  
Netherlands | [www.knmi.nl](http://www.knmi.nl)